ISIJ International, Vol. 49 (2009), No. 12, pp. 1938–1944

The Effect of S and Mn on the High-temperature Oxidation and Scale Spallation Behavior of Low-carbon Steels

Shigenari HAYASHI,[1] Takeshi SEKIMOTO,[2] Kazuhiko HONDA,[3] Takeshi KINOSHITA,[4] Kazuaki TANAKA,[4] Kohsaku USHIODA,[5] Toshio NARITA[1] and Shigeharu UKAI[1]

1) Division of Materials Science and Engineering, Graduate School of Engineering, Hokkaido University, N13, W8, Kitaku, Sapporo 060-8628 Japan. E-mail: hayashi@eng.hokudai.ac.jp
2) Formerly Division of Materials Science and Engineering, Graduate School of Engineering, Hokkaido University, N13, W8, Kita-ku, Sapporo 060-8628 Japan. Now at Sumitomo Metal Industries, Ltd., Kashima Steel Works, 3, Hikari, Kashima 314-0014 Japan. 3) Kimitsu R&D Lab., Technical Development Bureau, Nippon Steel Corp., Kimitsu 299-1141 Japan.
4) Kimitsu Works, Nippon Steel Corp., Kimitsu 299-1141 Japan. 5) Technical Development Bureau, Nippon Steel Corp., Futtsu 293-8511 Japan.

(*Received on July 14, 2009; accepted on September 7, 2009*)

Early-stage oxidation behavior in air of low-carbon steels with and without S and Mn additions was investigated in terms of oxidation kinetics and scale spallation in a temperature range of 900 to 1 150°C. S and Mn did not appear to affect the growth rate of oxide scales within the given oxidation time, ~30 min, however it was found that S significantly enhanced oxide scale spallation. Scale spallation occurred only on the S doped steels oxidized at temperatures more than 1 000°C when the thickness of oxide scale exceeded about 120 μm. This scale spallation was confirmed to occur during cooling after the given oxidation time. GD-OES analysis revealed that a significant amount of S enrichment occurred at the oxide/steel interface, which was around 1 mass% on 100 ppm S steel after 120 s of oxidation at 1 150°C. Such sulfur enrichment was speculated to be due to accumulation of rejected S from surface recession during the high-temperature oxidation. Observation of the steel surface after complete removal of the oxide scale by quenching the steels into liquid nitrogen clearly indicates the formation of eutectic Fe–FeS structure at scale/steel interface, resulting from a liquid phase formation above 1 000°C. Formation of sulfide, and therefore a liquid phase at higher temperature, greatly affected oxide scale spallation.

KEY WORDS: S effect; hot-rolled steel; scale spallation; Fe–FeS eutectic reaction.

1. Introduction

Commercial steel plates are manufactured by hot-rolling process at higher temperatures in air. In the hot-rolling process, a slab is initially heated to around 1 200°C in a reheating furnace, followed by hot-rolling down to the desired thickness by means of hot strip mills at temperatures above 900°C in air. During such a high temperature manufacturing process, iron oxide scales develop on the slab and steel plate. Since the oxide scale is rolled simultaneously with the steel substrate, non-uniform distribution of the oxide scale can often be the origin of formation of various surface defects of steel plates. Such defects result in rejection of the final steel products due to poor surface appearance. Therefore understanding the oxidation behavior of steels and spallation behavior of the oxide scale during hot-rolling and controlled scale removal processes are some of the most important issues in the steel making industry.

The oxide scale formed during the high temperature process is usually removed from the steel surface by means of so-called "de-scaling process" which are hydraulic and/or high-pressure water jet spray descalers. Oxide scale characteristics including mechanical properties, microstructure, and scale adhesion on a steel substrate significantly affect the surface condition after the de-scaling process. Oxide scale properties and adhesion depend upon the steel composition, temperature of reheating and rolling, and the thickness of oxide scale. Even very small amounts of impurities and intentionally added elements such as C, Si, Mn, P, and S have been observed to affect oxide scale properties.[1)]

Several studies have been conducted[1,2–5)] on the effect of those elements on the oxidation behavior of low-carbon steels or iron, however much attention has been paid to clarify the effect of Si,[6–8)] due to its stronger affinity with oxygen. S is known to have a detrimental effect on scale adhesion on oxidation resistant alloys and coatings which form a protective oxide scale of Al_2O_3 or Cr_2O_3. This detrimental effect attributed to S segregation at the scale/alloy interface, which weakens the interfacial strength. In the steel production field, it has long been recognized that oxide scales can be easily removed by the de-scaling process if steels contained sufficiently high levels of S. One possible explanation for this S effect on the scale spallation on steel is formation of a liquid phase at the scale/steel interface by FeO/FeS eutectic reaction.[4,5)] However, the reason for this favorable effect of S on the de-scaling process, *i.e.* en-

Table 1. Compositions of the steels used in this study (mass%).

Sample	C	Si	Mn	P	S	Al
base	0.0018	0.008	0.01	0.001	0.0002	0.031
30S	0.0007	0.006	0.01	0.001	0.0027	0.028
100S	0.0008	0.007	0.01	0.001	0.01	0.024
100SM	0.0008	0.006	0.12	0.001	0.01	0.022

hanced spallation behavior of oxide on S-containing steels, has not been systematically investigated.

In this study, we investigated the effect of S as well as Mn additions on the oxidation and scale spallation behavior of low-carbon steel, and tried to clarify the beneficial reasons why S addition makes the scale removable easier.

2. Experimental Procedure

Low carbon steels with three different S contents of 2, 30, 100 ppm (in mass%), and one with 100 ppm S and 0.12% Mn were melted in a vacuum furnace. The compositions of the steels used in this study are shown in **Table 1**. The ingots were then hot-rolled at the temperature range 940 to 1 050°C down to a final thickness of about 4 mm. 15 mm×15 mm square shaped oxidation samples were cut from the hot-rolled plates. Surface oxide scale formed during the above mentioned process was removed using 80-grit SiC abrasion paper, and then ground to a 1 200-grit finish. All samples were then ultrasonically degreased in acetone and kept in a desiccator for at least 24 h prior to oxidation testing.

Oxidation experiments were performed using an open, vertical furnace equipped with a timer-controlled, sample-elevation system as shown in **Fig. 1**. Samples were hooked to an Al_2O_3 rod and then automatically raised into the furnace hot zone, which was kept at 900, 1 000, or 1 150°C. After oxidation for a given time, the samples were automatically lowered to a position below the furnace tube and allowed to air-cool to room temperature. The temperatures were measured using an R-type thermocouple located adjacent to the sample surface. **Figure 2** shows sample temperature profiles with time. For all oxidation temperatures, the time taken for near the sample surface to reach to the furnace setting temperature was approximately 120 s. On 1 150°C exposures, temperatures near the surface increased over the furnace temperatures due to heat evolution of oxidation reaction. Several samples were dropped into liquid-nitrogen without using the sample elevation unit, just after the given isothermal oxidation time in order to protect the steel surface during cooling from air if the oxide scale was spalled off. The cooling rate of the samples in the case of liquid–nitrogen quenching was confirmed to be similar to the samples cooled in air.

Sample mass was measured before and after each oxidation test using an analytical balance. Cross-sections were observed using an optical and scanning electron microscope. Element distributions were measured as a function of depth from the sample surface using glow discharge optical emission spectroscopy (GD-OES). Surface morphology and element mapping of the scale/steel interface after removal of oxide scale were examined using a SEM equipped with EDS.

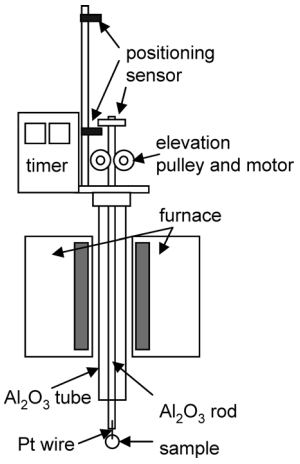

Fig. 1. Oxidation apparatus used in this study.

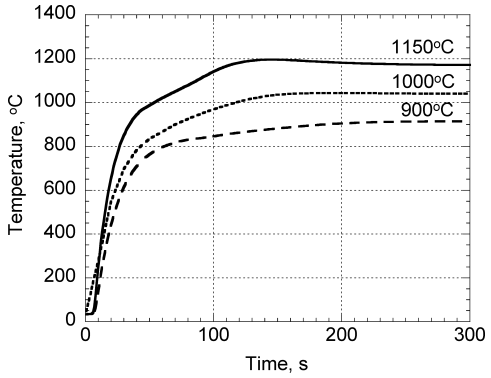

Fig. 2. Temperature profiles neat the sample surface during heating.

3. Results

3.1. Oxidation Kinetics

Figure 3 shows the oxidation kinetics of the steels at 900, 1 000, and 1 150°C. Oxidation was slow during the initial 60 s of heating but rapidly increased after 120 s of heating, which corresponds to the time for the samples to reach furnace temperature (see Fig. 2). For longer oxidation, the oxidation rate decreased and followed parabolic kinetics. The oxidation kinetics were similar for all samples at each temperature, and few effects of S and Mn on scale growth kinetics were observed. However, after 300 s of oxidation at 1 150°C, large difference in oxidation mass gains, 56.1 mg/cm^2 for 100 ppm S and 34.9 mg/cm^2 for 30 ppm S steels, were observed. This could be due to small differences in oxidation time causing large differences in mass gain, since the growth rate of Fe oxide scale was very fast particularly at higher oxidation temperatures, and 300 s at 1 150°C was within the initial fast rate of oxidation. Therefore when the oxidation rate decreased after longer expo-

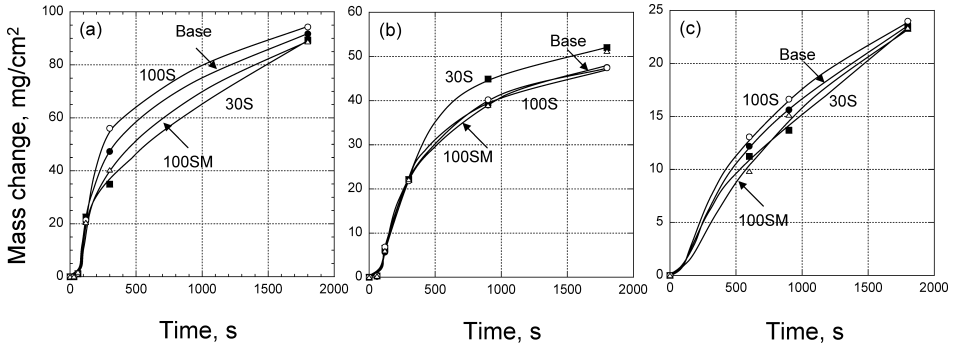

Fig. 3. Oxidation kinetics of the steels during heating and followed by isothermal oxidation in air. (a) 1 150°C, (b) 1 000°C, and (c) 900°C.

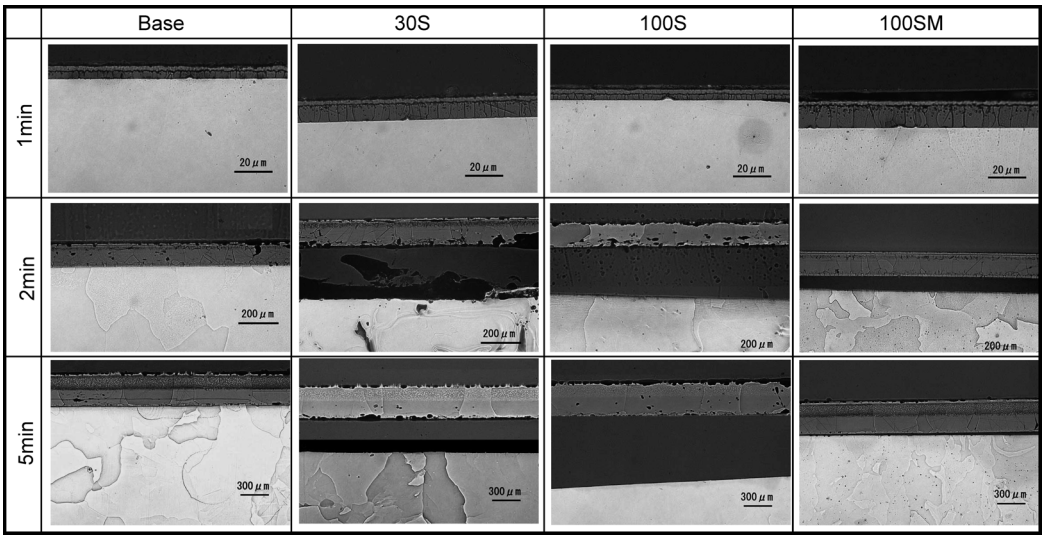

Fig. 4. OM cross-sections of steels after oxidation at 1 150°C.

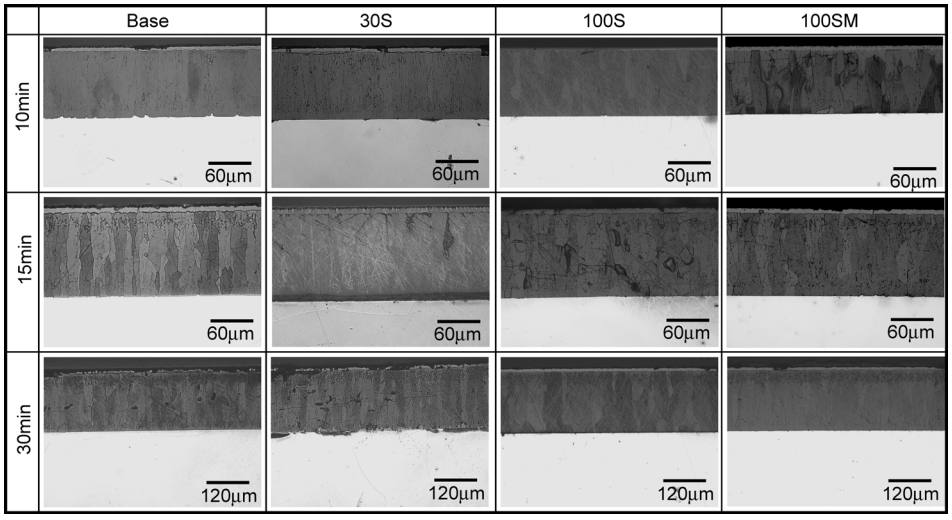

Fig. 5. OM cross-sections of steels after oxidation at 900°C.

sure time for 1800s, the differences in mass gain of each sample became smaller.

3.2. Scale Spallation Behavior

Figures 4 and **5** show optical cross-sectional microstructures of steels after different exposure times at 1 150 and 900°C. Oxide scales were consisted of thin Fe_2O_3, Fe_3O_4 and thicker FeO, in this order, from the outer surface. Fe_3O_4 precipitates, which formed during cooling, were also observed in the outer region of FeO scale. Spallation of oxide scale was observed on S containing steels after 120 s at 1 150°C, but oxide scales on the non-S containing steel never spalled off. Oxide scale spallation was also observed on S containing steels at 1 000°C after 300 s of oxidation, however at 900°C no spallation was observed to occur on any of the steels, even those containing S, within the oxida-

tion time used in the present study, ~30 min.

Oxide scale/steel interfaces on all steels were very flat, and scale spallation seemed to occur at the scale/steel interface. No apparent oxide formation was observed on the steel surface after scale spallation from the optical cross-sections, and the spalled oxide scale consisted of Fe_2O_3, Fe_3O_4, and FeO with the same order and thickness ratio as the non-spalled scales. This result indicates that scale spallation occurred when sample temperature cooled sufficiently to prevent re-oxidization of the surface of steels. **Figure 6** shows a spallation map relating to steel S content, oxidation time, and oxide scale thickness at different temperatures. The critical oxide scale thickness for scale spallation to occur was found to be about 120 μm. However oxide scales did not spall off at 900°C, even though the scale exceeded this critical thickness after a longer oxidation time.

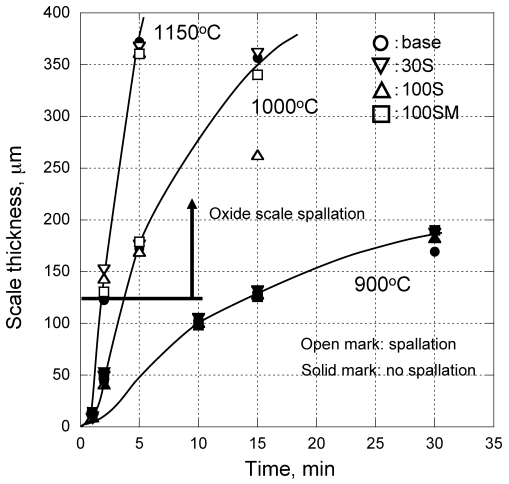

Fig. 6. Spallation map of the oxide scale formed on the steels with/without S and Mn additions at different temperatures.

3.3. Distribution of Each Element by GD-OES Analysis

Figures 7 and **8** show representative distributions of each element in the oxide scales after 30 and 60 s of heating at 1 150°C measured by GD-OES. At those heating times, oxide scales were still well attached to the steels. Si and Al enrichments were observed near the scale/steel interface on all steels. Apparent S enrichment was also observed near the interface of S-containing steels particularly after 60 s of heating. S content in the enriched layer increased with increase in both steel S content and oxidation time. Careful examination of profiles of Si, Al and S revealed that the enrichment of those elements occurred in the order of Si, Al, and S, toward the steel substrate, indicating that S enriched at Al-rich oxide layer/steel interface. Mn in S–Mn co-doped steel was distributed widely in the FeO layer, and its content in the FeO layer was similar to in the substrate. A small Mn enrichment was also observed at the scale/steel interface accompanying the enrichment of S. This Mn profile indicated that Mn and S co-exist at the scale/steel interface, however, no apparent effect of Mn on the distribution of S or spallation behavior of oxide scale was observed. Similar profiles for each element were also observed at 1 000°C, but S contents at the interface for the same oxidation time was lower than at 1 150°C. The oxide scale formed at 900°C for 10 min of oxidation was too thick to analyze by GD-OES, therefore no profiles of elements could be obtained in the present study.

Figure 9 shows the S profiles of 30S and 100S steels after 120 s of heating following by quenching in liquid nitrogen. As mentioned previously, oxide scales were completely spalled off from the steels at this oxidation time, so GD-OES measurements were conducted on the steel surface without oxide scale. Even after scale spallation, several microns of Fe oxide scale was detected. However, S con-

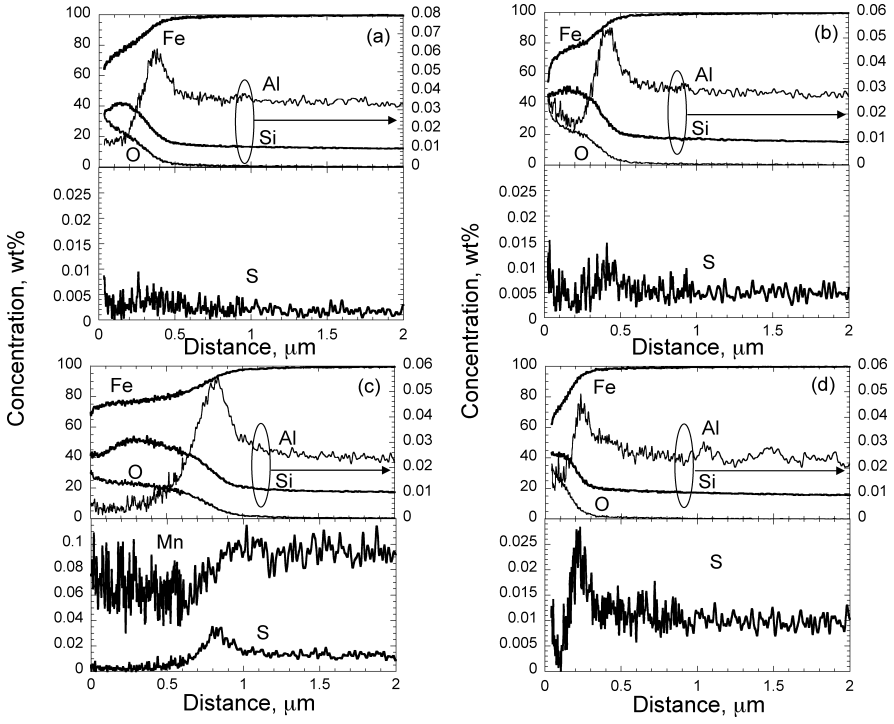

Fig. 7. GD-OES profiles of each element at 1 150°C for 30 s. (a) Base, (b) 30S, (c) 100SM, and (d) 100S.

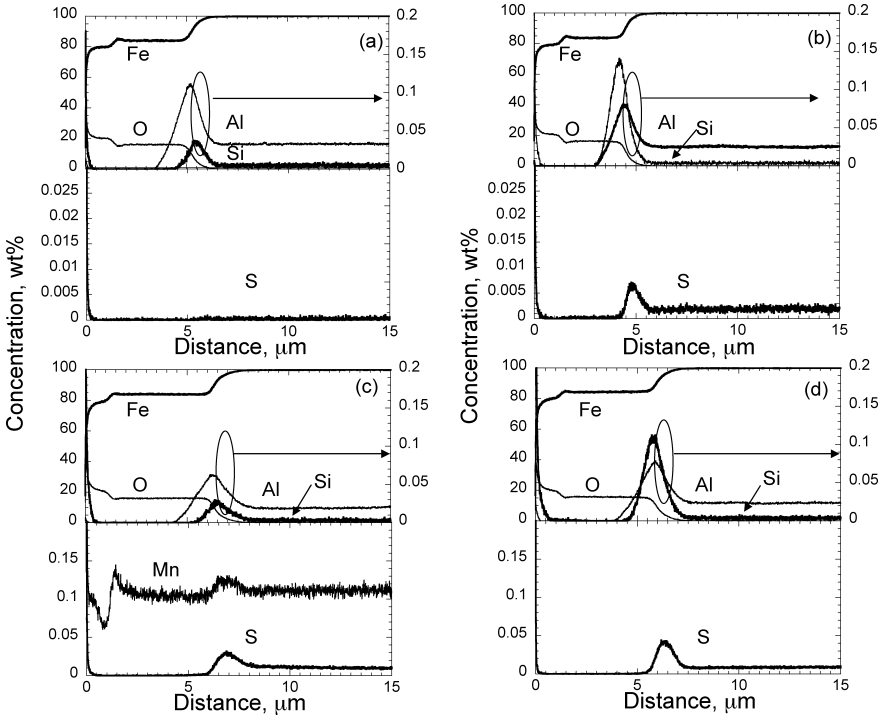

Fig. 8. GD-OES profiles of each element at 1 150°C for 60 s. (a) Base, (b) 30S, (c) 100SM, and (d) 100S.

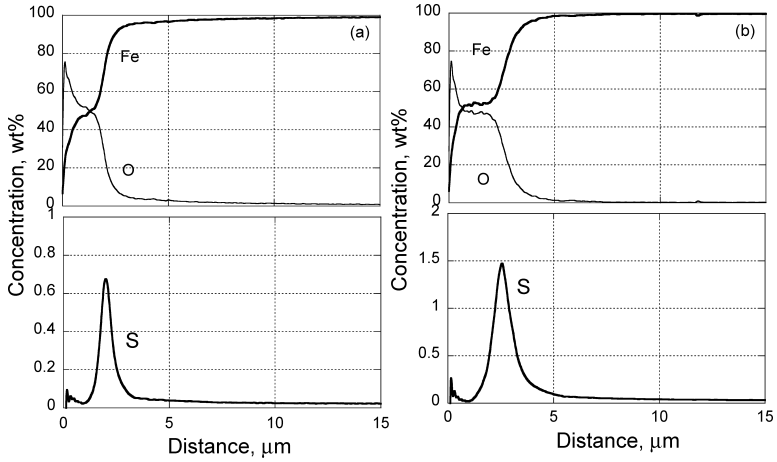

Fig. 9. GD-OES profiles of the surface after scale spallation of (a) 30S and (b) 100S steels at 1 150°C for 120 s.

tents at the scale/steel interface of 30S and 100S steels were found to increase significantly to about 0.7 mass% and 1.5 mass%, respectively.

4. Discussion

Four steels with and without different S and Mn contents were oxidized at 900, 1 000, and 1 150°C in air. S and Mn did not appear to affect oxidation kinetics at any temperature in the given oxidation time used in the present study. S was found to enhance scale spallation significantly, particularly at the higher temperatures of 1 000 and 1 150°C, however scales formed at 900°C on all steels never spalled within the range of oxidation time, ~30 min, in this study. Scale spallation on S-containing steels occurred when scale thickness exceeded about 120 μm, independent of the oxidation temperature and S content. The addition of Mn was found to have no effect for this critical thickness for scale spallation. In order to determine more accurate critical thickness and to examine the effect of S content, more detailed study with smaller increments in oxidation time is required. Apparent S enrichment was observed at the scale/steel interface even after very shot times of heating, ~60 s. S content at the scale/steel interface increased with increasing with steel S content and oxidation time. Mn was also found to enrich at the scale/steel interface accompanying S-enrichment, suggesting that Mn and S co-existed at the interface. These results strongly suggest that the scale spallation was enhanced by S enrichment at the interface at temperatures above 1 000°C.

The detrimental effect of S on the protective oxide scale spallation behavior of heat resistant alloys is widely reported, and is often attributed to S segregation to the interface.[9,10] S content at the interface was previously measured by Auger analysis, for example on NiAl alloy with 3–4 ppm S after 10 h of oxidation at 1 000°C was reported to be about 2 at%.[11] The thickness of the S segregated layer on such oxidation resistant alloys was also estimated to be very

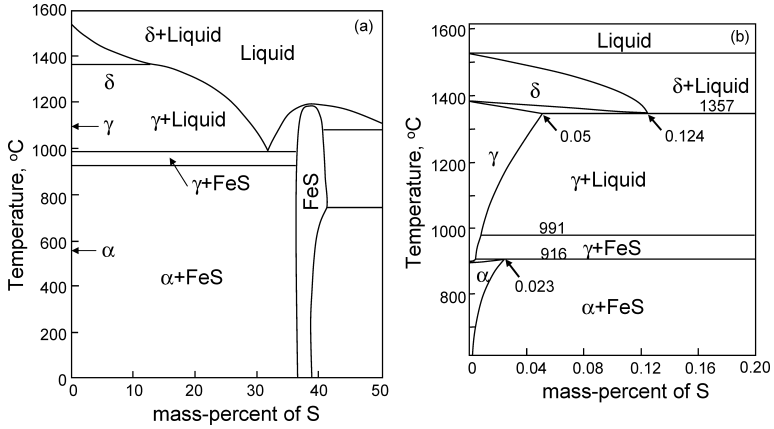

Fig. 10. Fe–S binary phase diagram. (b) is low sulfur region up to 0.2 mass% sulfur.

thin, about four atomic layers.[11] In the present study, however, the thickness of S enriched layer on 100S steel after 120 s of heating estimated from GD-OES analysis was about 1 μm (see Fig. 9), and is too thick to be caused by S diffusion from the substrate due to segregation energy, as proposed for heat resistant alloys.

4.1. Steel Recession and S-enrichment

For steel oxidation, Fe and S in the steel oxidized simultaneously when steels were exposed in air at high temperatures. But when an Fe-oxide scale developed on the surface of the steel, FeO/Fe equilibrium was established at the scale/steel interface. At the oxygen potential of FeO/Fe equilibrium at the given temperatures, S in the steel cannot be oxidized, since the standard Gibbs free energy change, $\Delta G°$, of SO_2 formation is much higher than that of FeO. Moreover free energy change for the formation of SO_2 in the present study at such a low oxygen potential at the interface should be positive, since S content in the steel is very low, ~100 ppm. Consequently S should not be oxidized and be rejected to the substrate with the progress of oxidation due to steel consumption, *i.e.* surface recession, and rejected S then diffuses into the steel substrate. However, if the consumption rate of steel is much faster than S diffusion into substrate, S will be enriched at the interface. In the present study, total thickness of metal recession after initial 5 min of heating to 1 150°C, calculated from Fig. 3, was 220 μm. This is much thicker than the diffusion depth of S expected from its diffusivity in γ-Fe, 1.2×10^{-8} cm^2/s.[12,13] Therefore S content at the interface can be calculated from just the steel recession, without S inward diffusion. Thickness of the S-enriched layer, 1 μm, was taken to be the width between half-maximum values of the GDS profile of 100 ppm S steel after 2 min of oxidation in Fig. 9. Using the thickness and calculated sulfur content of the recessed region gives a sulfur content in the 1 μm S-enriched layer of 1.6 mass%, which agrees roughly with the GD-OES result shown in Fig. 9.

Mn is known to form MnS and decrease the activity of sulfur in a steel substrate, so it was expected to suppress the formation of FeS at the interface, which can cause liquid phase formation due to the eutectic reaction of Fe/FeS as discussed in the next section. Mn enrichment was also observed at the scale/steel interface suggesting the formation of MnS. However Mn has a stronger affinity for oxygen than Fe, and MnO is much more stable than MnS, therefore MnS can be oxidized below the FeO scale to form MnO, releasing S at the interface. This could be one of the reasons why Mn has no effect on suppression of S-enrichment at the interface, and on scale spallation behavior.

4.2. Liquid Phase Formation at the Interface

S content at the scale/steel interface of 30S, about 0.7 mass%, and 100S, 1.5 mass%, steels after 120 s of heating at 1 150°C obtained in this study are much higher than the solubility limit of S in γ-Fe at 1 150°C, which is less than 300 ppm from the Fe–S binary phase diagram[14] shown in **Fig. 10**. At such high S content, FeS must be formed and may react with Fe to form a liquid phase due to the Fe–FeS eutectic reaction at 988°C. Moreover, the lower ternary eutectic reaction of Fe–FeO–FeS at 910°C[15] could also possibly enhance liquid phase formation. With increasing oxidation time, the amount of liquid phase increases due to the increasing steel consumption, and thus increasing S content. It is reasonable to think that a liquid phase could cause the scale/steel interface weaken, finally resulting in oxide scale spallation. A supporting result for the formation of a liquid phase is shown in **Fig. 11**. This 100 ppm S steel sample was quenched into liquid nitrogen after 2 min of heating at 1 150°C. The surface of the specimen was protected against re-oxidation by nitrogen gas after scale spallation during cooling, and sulfides were expected to remain on the surface. The surface of the steel was relatively smooth, and colonies of small particles were distributed on the surface. EPMA element mapping clearly indicates those particles are S-rich, but no S was detected on the rest of the smooth area. This surface morphology and EPMA mapping shown in Fig. 11 suggests the formation of a Fe–FeS eutectic structure, which in turn can cause liquid phase formation at higher temperatures.

This liquid phase formation may not be the actual trigger to cause scale spallation. Residual stresses within the oxide scale developed during cooling due to CTE mismatch and/or volume change of the substrate due to γ–α phase transformation are also possible sources for causing scale spallation. Since no scale spallation was observed on the steel without S addition, or the samples oxidized at temperature lower than the eutectic temperature of 988°C, it appears that S decreases the interface strength due to liquid phase formation by Fe–FeS eutectic reaction.

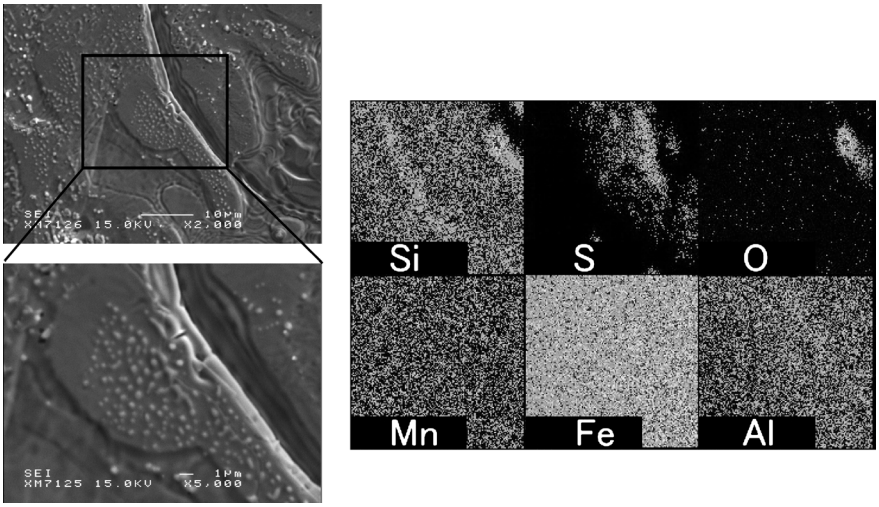

Fig. 11. Surface morphologies and elemental map of the steel surface of 100S after oxidation at 1 150°C for 120 s followed by scale spallation in liquied nitrogen.

5. Conclusion

The oxidation behavior of low carbon steels with and without 30 ppm, 100 ppmS and 100 ppmS+0.12 mass%Mn at 900 to 1 150°C was investigated, and the effect of S and Mn on the scale spallation was discussed. Results obtained may be summarized as follows.

(1) S and Mn did not affect oxidation kinetics at the temperatures used in this study.

(2) S enhanced scale spallation significantly at the higher temperatures of 1 000 and 1 150°C, however the oxide scale never spalled at 900°C. Mn did not affect scale spallation behavior.

(3) Scale spallation occurred when oxide thickness exceeded about 120 μm, and this thickness was independent of oxidation temperature.

(4) S enrichment occurred at the scale/steel interface, and this was attributed to rejection of S from the recessed substrate during oxidation. S content at the interface was found to be about 1.5 mass% in the case of 100 ppmS steel after 2 min of heating at 1 150°C.

(5) Liquid phase formation was confirmed at the scale/steel interface, and this may cause enhanced scale spallation due to decreasing the interfacial strength.

REFERENCES

1) R. Y. Chen and W. Y. D. Yuen: *Oxid. Met.*, **59** (2003), 433.
2) D. Genéve, D. Rouxel, P. Pigeat, B. Weber and M. Confente: *Appl. Surf. Sci.*, **254** (2008), 5348.
3) T. Fukagawa, H. Okada and H. Fujikawa: *Tetsu-to-Hagané*, **83** (1997), 305.
4) T. Mishima and M. Sugiyama: *Tetsu-to-Hagané*, **30** (1946), 231.
5) T. Fukagawa, H. Okada and Y. Maehara: *Tetsu-to-Hagané*, **81** (1995), 559.
6) M. Fukumoto, S. Hayashi, S. Maeda and T. Narita: *Tetsu-to-Hagané*, **85** (1999), 878.
7) M. Fukumoto, S. Hayashi, S. Maeda and T. Narita: *Tetsu-to-Hagané*, **86** (2000), 526.
8) S. Taniguchi, K. Yamamoto, D. Megumi and T. Shibata: *Mater. Sci. Eng.*, **A308** (2001), 250.
9) Y. Ikeda, K. Nii and K. Yoshihara: *Trans. Jpn. Inst. Met. Suppl.*, **24** (1983), 207.
10) D. G. Lees: *Oxid. Met.*, **27** (1989), 75.
11) P. Y. Hou: *Annu. Rev. Mater. Res.*, **38** (2008), 275.
12) V. V. Mural' and A. P. Fokin: *Met. Sci. Heat Treat.*, **20** (1978), 501.
13) A. Hoshino and T. Araki: *Tetsu-to-Hanagé*, **56** (1970), 252.
14) A. F. Guillermet, M. Hillert, B. Jansson and B. Sundman: *Metall. Trans. B*, **12B** (1981), 745.
15) V. D. Eisenhüttenleute ed., Schlackenatlas: Verlag Stahleisen M.B.H., Düsseldorf., (1981), 43.